

## Far infrared spectroscopy of $\text{Pb}_{1-x}\text{Eu}_x\text{Te}$ epitaxial layers

E. S. Zhukova, N. P. Aksenov, and B. P. Gorshunov

*A.M. Prokhorov General Physics Institute, Russian Academy of Sciences, Vavilov Str., 38, 119991 Moscow, Russia*

Yu. G. Selivanov and I. I. Zasavitskiy

*P.N. Lebedev Physical Institute, Russian Academy of Sciences, Leninskii prospect 53, 119991 Moscow, Russia*

D. Wu and M. Dressel

*1. Physikalisches Institut, Universität Stuttgart, Pfaffenwaldring 57, 70550 Stuttgart, Germany*

(Received 2 September 2010; published 2 November 2010)

Transmission and reflection coefficients of epitaxial layers of solid solutions  $\text{Pb}_{1-x}\text{Eu}_x\text{Te}$  ( $0 \leq x \leq 0.37$ ) on  $\text{BaF}_2$  and Si substrates are measured in a wide frequency range from 7 to  $4000 \text{ cm}^{-1}$  at temperatures between 5 and 300 K. Although several phonon and impurity absorption lines of the substrate and buffer layers dominate the absorption spectra, a local  $\text{Pb}_{1-x}\text{Eu}_x\text{Te}$  mode is observed around  $110$  to  $114 \text{ cm}^{-1}$ . In addition, a soft transverse-optical phonon mode of  $\text{Pb}_{1-x}\text{Eu}_x\text{Te}$  is detected with the frequency decreasing from  $32$  to  $18 \text{ cm}^{-1}$  upon cooling from room temperature to 5 K.

DOI: [10.1103/PhysRevB.82.205202](https://doi.org/10.1103/PhysRevB.82.205202)

PACS number(s): 78.30.Hv, 71.20.Eh

### I. INTRODUCTION

Physical properties of europium chalcogenides  $\text{EuX}$  ( $X = \text{O}, \text{S}, \text{Se}, \text{Te}$ ), which form a separate class of magnetic semiconductors, are well described in literature.<sup>1–3</sup> Recently growing interest to these compounds was stimulated by promising applications of corresponding solid solutions for manufacturing of semiconductor heterostructures with effective electronic and optical confinement<sup>4–6</sup> and of highly reflecting Bragg mirrors<sup>7</sup> for the mid-infrared (IR) spectral range. Such mirrors are used in IR vertical cavity surface emitting lasers<sup>7</sup> and for highly selective IR resonant cavity enhanced detectors.<sup>8</sup>

The optical properties of  $\text{Pb}_{1-x}\text{Eu}_x\text{Te}$  solid solutions are not well studied. First photoluminescence experiments<sup>4</sup> have shown that the band gap  $E_g$  of the compound increases strongly and in a nonlinear fashion with the increasing Eu content. Yuan *et al.*<sup>9</sup> studied the dispersion of refraction and extinction coefficients of  $\text{Pb}_{1-x}\text{Eu}_x\text{Te}$  ( $0 < x < 0.05$ ) at energies above and below  $E_g$  ( $\nu = E_g/ch \sim 1000\text{--}5000 \text{ cm}^{-1}$ ;  $c$ —velocity of light and  $h$ —Planck's constant) at temperatures 5–300 K. In Ref. 10 oblique incidence transmission spectra are reported; it was found that the  $\text{Pb}_{1-x}\text{Eu}_x\text{Te}$  solid solution reveals a two-mode behavior with a local Eu mode in PbTe located at  $127 \text{ cm}^{-1}$ . Also, the energies of optical phonons in EuTe were determined at  $T=5 \text{ K}$ .

To obtain detailed information on interactions of Eu ions located in a crystal matrix of a IV–VI semiconductor, further optical experiments in the mid-IR and far IR spectral ranges are necessary. Here we present first results for transmission and reflection coefficients spectra of  $\text{Pb}_{1-x}\text{Eu}_x\text{Te}$  epitaxial layers grown on  $\text{BaF}_2$  and Si substrates, measured in a broad frequency range from ambient temperatures down to 5 K. Among strong impurity and phonon resonances in substrates and buffer layers, we can identify absorption lines in epitaxial layers around  $110\text{--}114 \text{ cm}^{-1}$  and softening of a transverse-optical phonon around  $20\text{--}40 \text{ cm}^{-1}$ .

### II. EXPERIMENT

Using molecular-beam epitaxy single-crystalline  $\text{Pb}_{1-x}\text{Eu}_x\text{Te}$  layers ( $0 \leq x \leq 0.37$ ) were grown on insulating freshly cleaved (111)  $\text{BaF}_2$  substrates.<sup>11</sup> This substrate material was chosen because the expansion coefficients of  $\text{BaF}_2$  and Pb–Eu chalcogenides are very similar; this enables us to cool down the sample several times without facing severe material problems. However,  $\text{BaF}_2$  has strong phonon and impurity absorption bands in the range  $100\text{--}600 \text{ cm}^{-1}$  and this makes it difficult to measure the transmissivity of the layers at these frequencies. For that reason, for Eu concentration  $x=0.07$  we have also used highly insulating (resistivity  $\rho \sim 50 \text{ k}\Omega \text{ cm}$ ) (111) Si substrates with  $\text{CaF}_2/\text{BaF}_2$  buffer layers<sup>12</sup> to ensure epitaxial growth according to the technique described in Ref. 13. The thickness of the  $\text{BaF}_2$  buffer layers was  $10\text{--}200 \text{ nm}$ .

Table I summarizes the characteristic parameters of our samples. X-ray analysis shows that the lattice constant of  $\text{Pb}_{1-x}\text{Eu}_x\text{Te}$  depends on the Eu concentration in a nonlinear way, in accordance with Ref. 4. Full width at half maximum of the X-ray rocking curves for the layers are about  $20'$ , indicating the misorientation of crystallites in the layers during partial relaxation of strain induced by the mismatch of the lattice parameters between substrate and layer.

Spectra of transmission  $\text{Tr}(\nu)$  and reflection  $R(\nu)$  coefficients were measured at frequencies  $\nu=7\text{--}4000 \text{ cm}^{-1}$  in the temperature range of 5–300 K. Two spectrometers were used: at terahertz frequencies ( $7\text{--}38 \text{ cm}^{-1}$ ) a quasi-optical spectrometer based on backward-wave oscillators with a frequency resolution  $\Delta\nu/\nu$  of about  $10^{-5}$ ;<sup>14</sup> in the infrared range ( $20\text{--}4000 \text{ cm}^{-1}$ ) a Bruker IFS-113v Fourier transform spectrometer. The spectra were combined and analyzed for each temperature. By comparing the results for PbEuTe layers on substrates with those for bare substrates we were able to assign the observed absorption lines either to PbEuTe, to the substrate, or to the buffer layer. To yield information on the line parameters the spectra were processed using Fresnel expressions for transmissivity/reflectivity of a two-layered

TABLE I. Composition and thickness of  $\text{Pb}_{1-x}\text{Eu}_x\text{Te}$  epitaxial layers and substrate materials. Absorption lines parameters:  $\Delta\epsilon$  is the dielectric contribution,  $\nu_0$  is the eigenfrequency, and  $\gamma$  gives the damping.

Material	Substrate	Epitaxial layer $\text{Pb}_{1-x}\text{Eu}_x\text{Te}$		Absorption line parameters		
	$d$ (mm)	$x$	$d$ ( $\mu\text{m}$ )	$\Delta\epsilon$	$\nu_0$ ( $\text{cm}^{-1}$ )	$\gamma$ ( $\text{cm}^{-1}$ )
(111) $\text{BaF}_2$	0.878	0	0.94			
(111) $\text{Si}/\text{CaF}_2$	0.36	0.06	0.6	0.9	112.6	16.2
(111) $\text{BaF}_2$	1.05	0.076	0.67	1.8	113	16.2
(111) $\text{Si}/\text{CaF}_2/\text{BaF}_2$	0.54	0.09	6	0.569	110	11.6
(111) $\text{BaF}_2$	0.748	0.25	4.33	0.4	110	8.05
(111) $\text{BaF}_2$	0.746	0.37	3.74	0.77	111.5	15.2

(film on a substrate) system with the following Lorentzian expression describing the dispersion of complex dielectric permittivity due to resonance absorption:<sup>15</sup>

$$\epsilon^* = \epsilon'(\nu) + i\epsilon''(\nu) = \frac{\Delta\epsilon\nu_0^2}{\nu\gamma + i(\nu_0^2 - \nu^2)}. \quad (1)$$

Here  $\epsilon'(\nu)$  and  $\epsilon''(\nu)$  are the real and the imaginary parts of the dielectric permittivity,  $\Delta\epsilon$  denotes the strength of the dielectric contribution of the absorption line,  $\nu_0$  is its eigenfrequency, and  $\gamma$  is the damping parameter. The calculated values of these parameters are listed in Table I.

### III. RESULTS AND DISCUSSION

Figure 1 shows typical spectra of transmission coefficient  $\text{Tr}(\nu)$  of an epitaxial layer  $\text{Pb}_{1-x}\text{Eu}_x\text{Te}$  ( $x=0.076$ ) on  $\text{BaF}_2$  substrate measured at  $T=10$  and 300 K. Oscillations below 40  $\text{cm}^{-1}$  and above 1000  $\text{cm}^{-1}$  come from interference of the radiation within the plane-parallel substrate (thickness of about 1 mm) and  $\text{PbEuTe}$  layer (thickness of about 1  $\mu\text{m}$ ), respectively. No substrate-related oscillations are seen in the spectra obtained on the Fourier spectrometer due to its lower frequency resolution ( $>2$   $\text{cm}^{-1}$ ). On the background of interference oscillations, absorption lines are seen as additional

features (minima). The broad minimum between 100 and 600  $\text{cm}^{-1}$  is connected with phonon and impurity absorption lines in  $\text{BaF}_2$  mentioned above and located between 200 and 600  $\text{cm}^{-1}$ .<sup>16,17</sup> The comparison of impurity absorption spectra with the calculated density of states evidences that the absorption at 127  $\text{cm}^{-1}$  is due to the low-energy  $T_2$  resonance of H ion.<sup>18</sup> The line at 145  $\text{cm}^{-1}$  corresponds to the two-phonon resonance process in  $\text{BaF}_2$ : at low temperatures the two-phonon absorption at the differential frequency is dominant,<sup>16</sup> in our case, it is the difference between longitudinal and transverse phonon frequencies,  $330-186=144$   $\text{cm}^{-1}$ .<sup>17</sup>

Below approximately 100  $\text{cm}^{-1}$ , where  $\text{BaF}_2$  becomes transparent, there are only two absorption lines related to  $\text{Pb}_{1-x}\text{Eu}_x\text{Te}$ . The first one is seen as a step around 33  $\text{cm}^{-1}$  at 300 K and as a minimum around 20  $\text{cm}^{-1}$  at 10 K. This line is present in  $\text{Pb}_{1-x}\text{Eu}_x\text{Te}$  layers grown on both  $\text{BaF}_2$  as well as silicon substrates, see Fig. 2, with basically the same line parameters. More details on the temperature evolution of the line are exhibited in Fig. 3. Figure 4 represents the temperature dependence of the line parameters: the frequency position, the dielectric contribution and the damping parameter. It is clearly seen that the line shifts toward low energies and that its damping decreases during cooling. The most pronounced shift happens in the temperature interval 130 K  $< T <$  200 K.

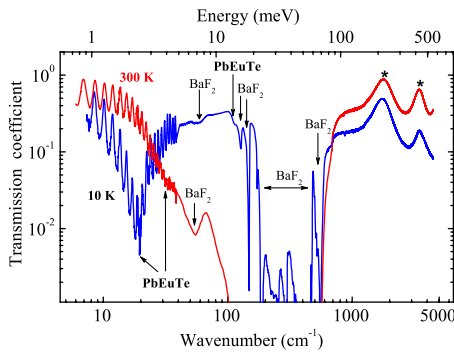


FIG. 1. (Color online) Transmission coefficient spectra of an epitaxial layer  $\text{Pb}_{1-x}\text{Eu}_x\text{Te}$  ( $x=0.076$ , thickness 0.67  $\mu\text{m}$ ) grown on  $\text{BaF}_2$  substrate (thickness 1.05 mm), measured at 300 and 10 K. Arrows show absorption lines in  $\text{BaF}_2$  and  $\text{PbEuTe}$ . Stars indicate maxima due to interference of radiation in the layer.

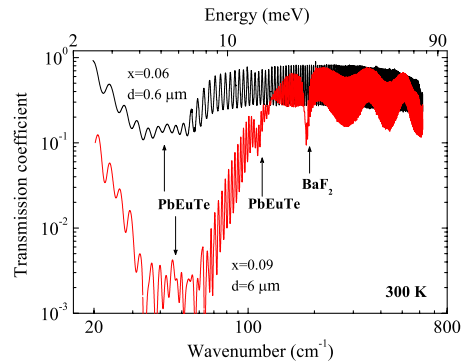


FIG. 2. (Color online) Transmission coefficient spectra of epitaxial layers  $\text{Pb}_{1-x}\text{Eu}_x\text{Te}$  with  $x=0.06$  (thickness 0.6  $\mu\text{m}$ ) and  $x=0.09$  (thickness 6  $\mu\text{m}$ ), grown on Si substrates (thickness 0.36 mm and 0.54 mm, respectively), measured at 300 K. Arrows show absorption lines in  $\text{PbEuTe}$  and in  $\text{BaF}_2$  buffer layer.

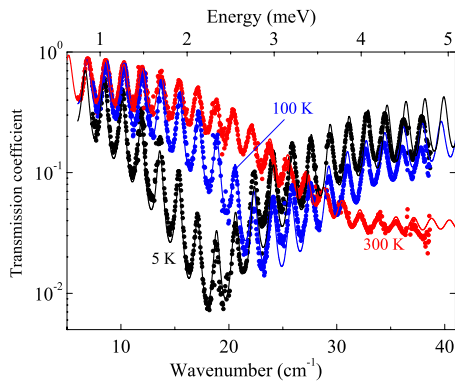


FIG. 3. (Color online) Transmission coefficient spectra of an epitaxial layer  $\text{Pb}_{1-x}\text{Eu}_x\text{Te}$  ( $x=0.076$ , thickness  $0.67 \mu\text{m}$ ) grown on  $\text{BaF}_2$  substrate (thickness  $1.05 \text{ mm}$ ) at different temperatures. Lines show least-square fits (see text). Temperature-dependent minimum corresponds to absorption due to a soft mode.

It is well known that ionic IV-VI semiconductors are characterized by large polarizability of the crystal lattice that leads to an increase in the dielectric permittivity at low temperatures and low frequencies. Such paraelectric behavior is most pronounced in  $\text{PbTe}$ . Adding small amounts of Ge can even cause a phase transition in a solid solution  $\text{PbGeTe}$ .<sup>19</sup> The first observation of a transverse  $\text{PbTe}$  optical phonon softening at frequencies  $5\text{--}100 \text{ cm}^{-1}$  and at low temperatures was reported in the reflectivity spectra of thin films on  $\text{BaF}_2$ .<sup>20</sup> According to our data obtained from the transmissivity measurements, as presented in Fig. 4, the softening of the transverse-optical mode in  $\text{Pb}_{0.93}\text{Eu}_{0.07}\text{Te}$  within experimental uncertainties is the same as in  $\text{PbTe}$ .

A relatively weak feature in the transmission coefficient spectra around  $110\text{--}114 \text{ cm}^{-1}$  indicates a second absorption line related to  $\text{PbEuTe}$ . This mode is shown in more details in Fig. 5 where the low-frequency ( $\nu < 200 \text{ cm}^{-1}$ ) spectra of  $\text{Pb}_{1-x}\text{Eu}_x\text{Te}$  layers with various Eu concentrations  $x$  grown on  $\text{BaF}_2$  are presented. With decreasing Eu concentration, the

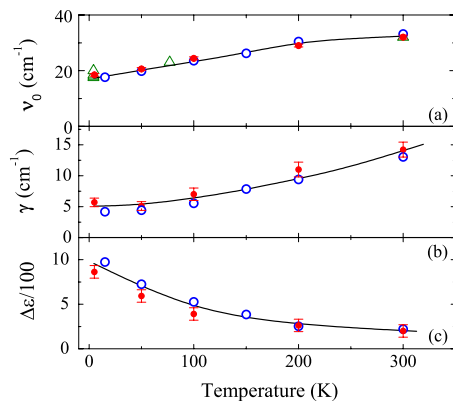


FIG. 4. (Color online) Temperature dependence of parameters of the soft mode observed in epitaxial layer  $\text{Pb}_{1-x}\text{Eu}_x\text{Te}$  ( $x=0.076$ ): (a) frequency position, (b) damping, and (c) dielectric contribution. Closed circles correspond to a layer on  $\text{BaF}_2$  substrate, open circles—on  $\text{Si}$  substrate. Triangles in panel (a) represent the data from Ref. 19 corresponding to the soft-mode position in  $\text{PbTe}$ . Lines are guide to the eyes.

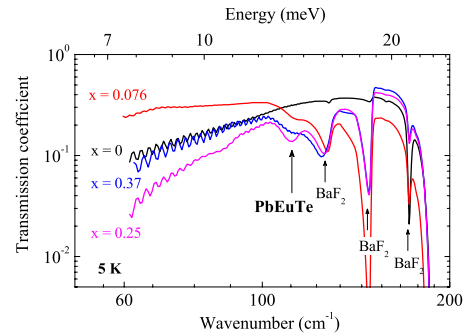


FIG. 5. (Color online) Transmission coefficient spectra of  $\text{Pb}_{1-x}\text{Eu}_x\text{Te}/\text{BaF}_2$  epitaxial layers with different concentrations  $x$  and thicknesses  $d$ :  $x=0$ ,  $d=0.94 \mu\text{m}$ ;  $x=0.076$ ,  $d=0.67 \mu\text{m}$ ;  $x=0.25$ ,  $d=4.33 \mu\text{m}$ ; and  $x=0.37$ ,  $d=3.74 \mu\text{m}$ .  $T=5 \text{ K}$ .

line shifts to higher frequencies, by about  $2 \text{ cm}^{-1}$  when the concentration changes from  $x=0.25$  to  $x=0.076$  (for solutions with  $x=0.25$  and  $x=0.37$  the line position is unchanged within experimental uncertainty).

We note that the frequency  $108 \text{ cm}^{-1}$  of the longitudinal-optical phonon in  $\text{PbTe}$  at low temperatures is slightly lower than the position of the feature seen in our spectra. We connect the absorption line at  $110\text{--}114 \text{ cm}^{-1}$  to another phase appearing in the form of disordered inclusions in the  $\text{PbEuTe}$  layer. As was shown in Ref. 21, this second phase contains  $\text{PbEuTe}$  with a Eu content smaller than in the layer itself. Typical sizes of inclusions were about  $1$  to  $10 \mu\text{m}$  depending on the sample growth procedure. These local inhomogeneities were first detected in photoluminescence spectra<sup>21</sup> where they lead to additional lines. The amount of this extra phase is not large ( $\sim 1\%$  of the total area of the layer) and this fact correlates with relatively low strength of the corresponding feature seen in our spectra.

In Fig. 6 we show the broadband spectra of real part  $n$  of the complex refractive index  $n^* = n + ik$  and of absorption coefficient  $\alpha = 4\pi k/\lambda$  ( $\lambda$  is the radiation wavelength) of  $\text{Pb}_{1-x}\text{Eu}_x\text{Te}$  layers with two different concentrations, obtained at room and liquid helium temperatures. Since the results obtained for  $\text{PbEuTe}$  layers grown on  $\text{Si}$  and  $\text{BaF}_2$

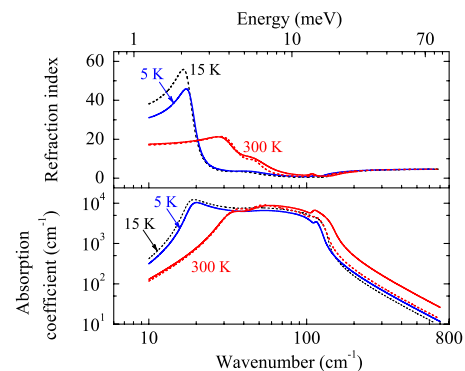


FIG. 6. (Color online) Spectra of refractive index  $n$  and absorption coefficient  $\alpha$  of two epitaxial layers  $\text{Pb}_{1-x}\text{Eu}_x\text{Te}$  with concentrations  $x=0.076$  (solid lines) and  $x=0.06$  (dashed lines), at three different temperatures. Solid and dashed lines correspond to layers grown on  $\text{BaF}_2$  and silicon substrates, respectively.

substrates perfectly agree we conclude that our findings are about the intrinsic behavior of PbEuTe solid solutions.

#### IV. CONCLUSION

Measurements of transmission and reflection coefficients spectra of  $\text{Pb}_{1-x}\text{Eu}_x\text{Te}$  ( $0 \leq x \leq 0.37$ ) epitaxial layers on  $\text{BaF}_2$  and Si substrates are performed at frequencies 7–4000  $\text{cm}^{-1}$  and temperatures 5–300 K. Besides the phonon and impurity absorptions in the substrates and buffer layers, absorption at 110–114  $\text{cm}^{-1}$  on local mode of PbEuTe solution is ob-

served. It originates from an additional phase which forms inclusions of a few micrometers in size. Softening of the transverse-optical phonon in PbEuTe is observed from 32 to 18  $\text{cm}^{-1}$  during cooling from 300 K down to 5 K.

#### ACKNOWLEDGMENTS

The work was supported by the Russian Foundation for Basic Research (Grant No. 09-02-91345-HHNO\_a) and by the Deutsche Forschungsgemeinschaft, DFG (Grant No. DR228/30-1).

- 
- <sup>1</sup>S. Methfessel and D. C. Mattis, in *Handbuch der Physik*, edited by S. Flügge (Springer-Verlag, Berlin, 1968), Vol. 18, p. 1.
- <sup>2</sup>S. Hüfner, *Optical Spectra of Transparent Rare Earth Compounds* (Academic Press, New York, San Francisco, London, 1978), p. 190.
- <sup>3</sup>P. Wachter, in *Handbook on the Physics and Chemistry of Rare Earth*, edited by K. A. Gschneidner, Jr. and L. R. Eyring (North-Holland, Amsterdam, 1979), Vol. 2, p. 507.
- <sup>4</sup>D. L. Partin, *IEEE J. Quantum Electron.* **24**, 1716 (1988).
- <sup>5</sup>M. Kriechbaum, P. Kocevar, H. Pascher, and G. Bauer, *IEEE J. Quantum Electron.* **24**, 1727 (1988).
- <sup>6</sup>I. I. Zasavitskii, E. A. de Andrada e Silva, E. Abramof, and P. J. McCann, *Phys. Rev. B* **70**, 115302 (2004).
- <sup>7</sup>W. Heiss, T. Schwarzl, J. Roither, G. Springholz, M. Aigle, H. Pascher, K. Biermann, and K. Reinmann, *Prog. Quantum Electron.* **25**, 193 (2001).
- <sup>8</sup>M. Arnold, D. Zimin, and H. Zogg, *Appl. Phys. Lett.* **87**, 141103 (2005).
- <sup>9</sup>S. Yuan, H. Krenn, G. Springholz, and G. Bauer, *Phys. Rev. B* **47**, 7213 (1993).
- <sup>10</sup>M. Aigle, H. Pascher, H. Kim, A. J. Mayur, E. Tarhan, A. K. Ramdas, G. Springholz, and G. Bauer, *Phys. Rev. B* **64**, 035316 (2001).
- <sup>11</sup>Yu. G. Selivanov, E. G. Chizhevskii, V. P. Martovitskiy, A. V. Knotko, and I. I. Zasavitskiy, *Inorg. Mater.* **46**, 1065 (2010).
- <sup>12</sup>Si substrates with  $\text{CaF}_2/\text{BaF}_2$  buffer layers were prepared at the Institute of Electronic Engineering and Industrial Technologies of Academy of Science of Moldova.
- <sup>13</sup>H. Zogg, S. Blunier, A. Fach, C. Maissen, P. Müller, S. Teodoropol, V. Meyer, G. Kostorz, A. Dommann, and T. Richmond, *Phys. Rev. B* **50**, 10801 (1994).
- <sup>14</sup>B. Gorshunov, A. Volkov, I. Spektor, A. Prokhorov, A. Mukhin, M. Dressel, S. Uchida, and A. Loidl, *Int. J. Infrared Millim. Waves* **26**, 1217 (2005).
- <sup>15</sup>M. Dressel and G. Grüner, *Electrodynamics of Solids* (Cambridge University Press, Cambridge, 2002).
- <sup>16</sup>D. R. Bosomworth, *Phys. Rev.* **157**, 709 (1967).
- <sup>17</sup>W. Kaiser, W. G. Spitzer, R. H. Kaiser, and L. E. Howarth, *Phys. Rev.* **127**, 1950 (1962).
- <sup>18</sup>J. A. Harrington and R. Weber, *Phys. Status Solidi B* **56**, 541 (1973).
- <sup>19</sup>E. Bangert, G. Bauer, E. J. Fantner, and H. Pascher, *Phys. Rev. B* **31**, 7958 (1985).
- <sup>20</sup>H. Burkhard, O. Bauer, and A. Lopez-Otero, *J. Opt. Soc. Am.* **67**, 943 (1977).
- <sup>21</sup>D. A. Pashkeev, Yu. G. Selivanov, F. Felder, and I. I. Zasavitskiy, *Semiconductors* **44**, 861 (2010).